SEISMIC EVALUATION OF THE HISTORIC CHURCH OF ST.NICHOLAS IN PIRAEUS BEFORE AND AFTER INTERVENTIONS

Constantine C. Spyrakos[1], Alessio Francioso[1], Panagiotis Kiriakopoulos[1], and Stavros Papoutsellis[1]

[1] Laboratory for Earthquake Engineering, School of Civil Engineering
National Technical University of Athens
Zografos 15700, Athens, Greece
e-mail: cspyrakos@central.ntua.gr

Keywords: historic masonry structure, in-situ testing, non-linear analysis, macroelements, strengthening interventions.

Abstract. *The construction of the church of St. Nicholas located in Piraeus dates back to 1839. Over the years the building has undergone several interventions until recent earthquakes caused serious damages to the structure. The damages are mainly attributed to the absence of particular provisions to sustain seismic loads. A detailed in-situ and laboratory testing of the masonry structure was carried out in order to search its geometry, the constructions details and the mechanical characteristics of the materials. Also, finite element analyses were performed in order to assess the current condition of the structure and its dynamic behavior. The capacity of the church was determined through linear global analysis and non-linear analysis with macroelements. Based on the results, strengthening interventions were proposed, using a combination of masonry consolidation techniques, carbon fiber reinforced materials (CFRP) and steel tie rods. The effectiveness of the strengthening is assessed through comparison of the analysis results before and after interventions.*

1   INTRODUCTION AND DESCRIPTION OF THE STRUCTURE

The construction of the church of St. Nicholas located in Piraeus dates back to 1839. It belongs to the type of cruciform temples with a form that follows the standards of the neoclassical style, distinguished by three monumental propylaea on the west, the north and south side, resembling the type of an ancient Corinthian temple [1].

Figure 1.   a) West façade and b) North façade of the church

The dimensions of the temple are 33.75m (depth) by 26.00m (length of the facade). The height of the walls is 16.52m. The height at the base of the dome reaches the 28m, while at the top the dome rises to 30m. The perimeter walls of the temple consist of three strata with a width of 1.30m. Generally the construction materials found in the building are stone, marble and tile.
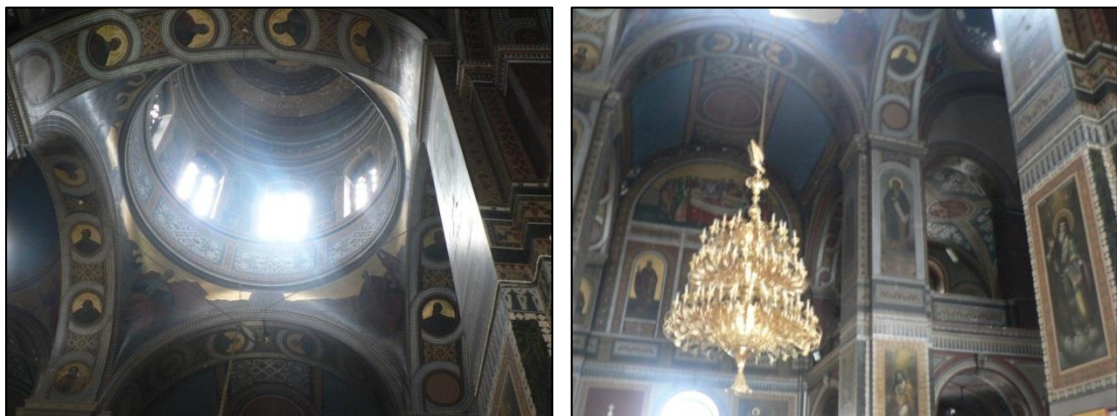

Figure 2.   a) Internal view of dome. b) Internal view over the temple

Over the years the building has undergone several modifications until recent earthquakes (the Alkyonides 1981 and the Athens 1999) caused serious damages to the structure. The damages are mainly attributed to the fact that no special consideration was given in the initial design for seismic loads. Cracks appear in many parts of the masonry structure and mainly at the intrados of arches and vaults in the longitudinal and transverse directions.

Because of its neighboring with the Piraeus harbor, just 100m away, the walls have suffered extensive weathering damage.
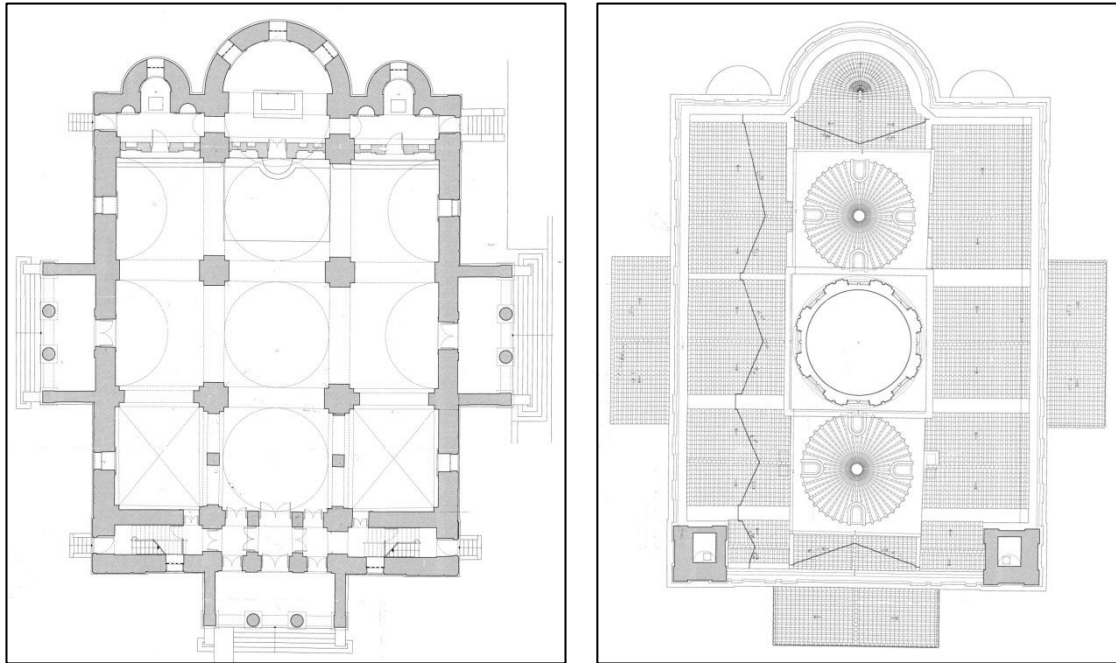
Figure 3.   a) Ground floor plan. b) Roof plan

Figure 4.   a) Through crack and detachment of lower drum at the southern part of the structure. b) Sliding of drum of a marble pillar caused by bombardment

2   IN SITU AND LABORATORY TESTING

Several tests were carried out in order to assess the mechanical characteristics of the masonry walls and the piers of the church. In-situ testing was performed at several locations

of the structure. Based on the collected measurements, the compressive strength of the stones was estimated to be:

$$f_{bc} = 40MPa$$

Drilled holes were opened in order to investigate by means of an endoscope the composition of the masonry walls along their thickness (Figure 5). The inspections revealed that the masonry walls were made of three-leaf masonry.

Figure 5. a) Area without plaster for inspection with endoscope. b) View inside the drilled hole

Mortar samples were analyzed following a three-step procedure: natural separation of mortar-stone, X-Ray diffraction and thermal analysis TG-DTG (Figure 6).
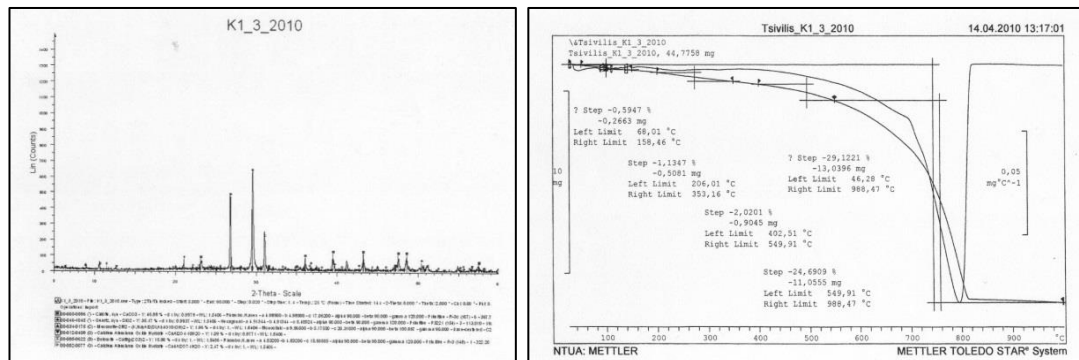

Figure 6. a) X-Ray analysis results. b) Thermal analysis results

The measurements and their analysis showed that: (i) the mortar contains natural hydraulic lime; (ii) the aggregate is a mixture of limestone, dolomitic and silica sands; (iii) the mortar contains muscovite.

The compressive strength of the mortar was estimated to be $f_{mc} = 1MPa$.

Ambient vibration tests were performed in order to measure the modes and natural frequencies of the church at its current state. The measurements were taken at three distinct positions: ground floor, mezzanine and dome level, along the principal directions of the church.

The analyses were performed using appropriate software that calculated transfer functions and Fourier spectra at different positions.

Table 1 presents the peaks of the Fourier spectra (see Figure 7) obtained from the ambient testing measurements.

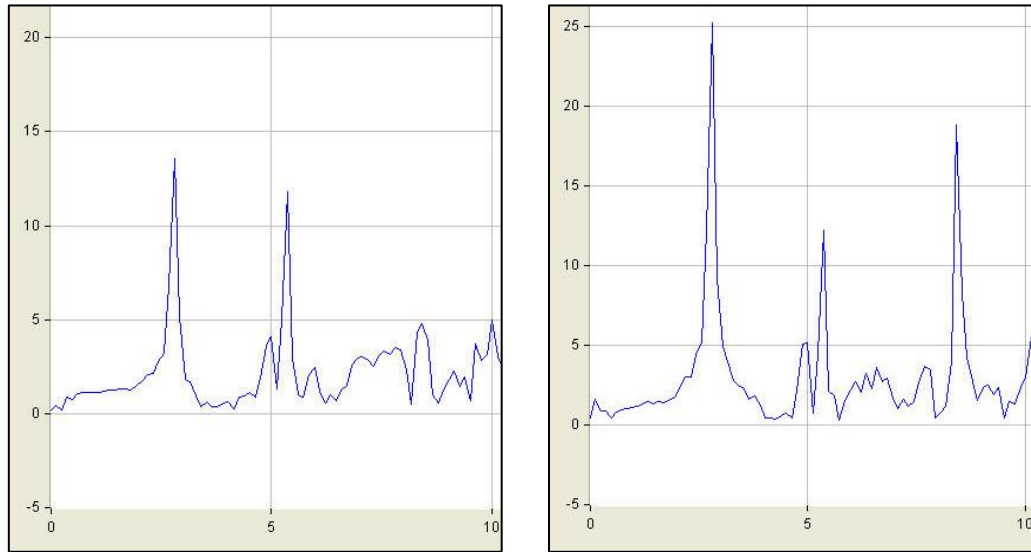|	Mode	Modal period (s)
Transverse direction X (N-S)	1	0.357
	2	0.187
Longitudinal direction Y (E-W)	1	0.329
	2	0.187

Table 1. Modal periods of the church

Figure 7. Transverse direction X (N-S): a) at mezzanine; b) at dome level

3 ANALYSIS OF THE CHURCH AT ITS CURRENT STATE

Two types of analyses were performed: a) global and b) local. With global analysis the structural response is studied with the aid of a finite element model considering that the structure behave as a whole, that is without developing any local mechanisms of failure.

The local analysis is performed only for the transversal frame that is directly loaded by the central dome; thus, one of the most vulnerable local load bearing systems of the church.

In order to calculate the compressive strength of the stone masonry, the following expression was used [2]:

$$f_{wc} = \frac{2}{3}\sqrt{f_{bc}} - a + \beta f_{mc}$$

(1)

where:

f_{bc} is the compressive strength of the stones;
f_{mc} is the compressive strength of the mortar;
α is a reduction factor (for masonry made of natural stone α = 1);
β is a factor that accounts for the mortar contribution on the masonry strength (for stone masonry β = 0.5).

The tensile strength and the modulus of elasticity were obtained from the masonry compressive strength according to the following expressions:

$$f_t = f_c / 10 \tag{2}$$

$$E = 1000 f_c \tag{3}$$

Table 2 presents the data used, as well as the results obtained from Equations (1 - 3).

Stones	Compressive strength	f_{bc}	40	N/mm^2
Mortar	Compressive strength	f_{mc}	1	N/mm^2
Masonry	Compressive strength	f_c	3.71	N/mm^2
	Tensile strength	f_t	0.37	N/mm^2
	Modulus of Elasticity	E	3710	N/mm^2
	Specific weight	W	22	kN/m^3

Table 2. Mechanical characteristics of masonry

3.1 Global analysis

The structural model and the global analysis of the structure were performed with the finite element software SAP2000 v.15 [3]. The stone masonry and marble elements were modeled with eight node solid elements with three degrees-of-freedom per node, while four-node shell elements were used to model the central dome. Frame elements were used for the proper connection and collaboration of solid and shell elements [4]. The final model consists of 42180 solids, 3350 shells, 96 frame elements and 63580 nodes, see Figure 8.
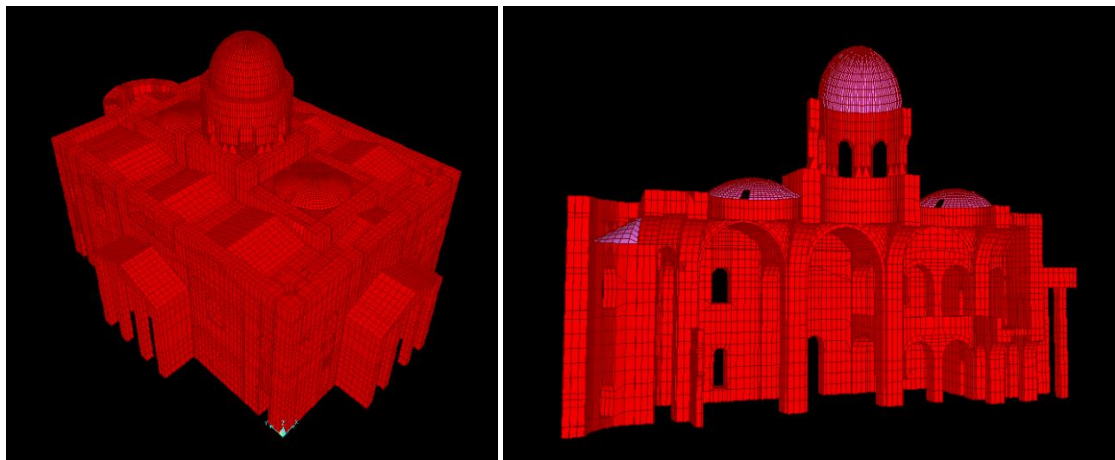

Figure 8. Three dimensional model: a) N-W view b) E-W section

The static and seismic analyses were performed applying the following loads:
a) the dead load of the masonry walls and the dome were automatically calculated by the program based on the dimensions of the structure and the specific weight. The tiles of the roof were considered as an additional weight equal to 0.9 kN/m^2
b) the live loads at the mezzanine were 5.0 kN/m^2.

A response spectrum analysis was performed according to Eurocode 8 [5, 6]. For the horizontal components of the seismic action the design response spectrum $S_d(T)$ is defined by the following expressions:

$$a_g = \gamma_I \cdot a_{gR} \tag{4}$$

$$0 \le T \le T_B : \ S_d(T) = a_g \cdot S \cdot \left[\frac{2}{3} + \frac{T}{T_B} \cdot \left(\frac{2,5}{q} - \frac{2}{3} \right) \right] \tag{5}$$

$$T_B \le T \le T_C : \ S_d(T) = a_g \cdot S \cdot \frac{2,5}{q} \tag{6}$$

$$T_C \le T \le T_D : S_d(T) \begin{cases} = a_g \cdot S \cdot \frac{2,5}{q} \cdot \left[\dfrac{T_C}{T} \right] \\ \ge \beta \cdot a_g \end{cases} \tag{7}$$

$$T_D \le T : \quad S_d(T) \begin{cases} = a_g \cdot S \cdot \frac{2,5}{q} \cdot \left[\dfrac{T_C T_D}{T^2} \right] \\ \ge \beta \cdot a_g \end{cases} \tag{8}$$

where T is the vibration period in sec, $a_{gR} = 0.16g$ is the design ground acceleration on soil type A, $\gamma_I = 1.2$ is the importance factor, $T_B = 0.15\,s$ is the lower limit of the period of the constant spectral acceleration branch, $T_C = 0.50\,s$ is the upper limit of the period of the constant spectral acceleration branch, $T_D = 2.00\,s$ is the value defining the beginning of the constant displacement response range of the spectrum, $S = 1.2$ is the soil factor, $\eta = 1$ is the damping correction factor, $q = 1.5$ is the behavior factor, $\beta = 0.2$ is the lower bound factor for the horizontal design spectrum.

For the vertical component of the seismic action the design response spectrum $S_d(T)$ is defined by Equations (4 - 8) replacing a_g with $a_{vgR} = 0.144g$ and adopting $T_B = 0.05\,s$, $T_C = 0.15\,s$, $T_D = 1.00\,s$, $S = 1$, respectively.

Table 3 presents the results of modal analysis for the first three modes as well as the corresponding modal participating mass ratios. A good correlation between the measured and calculated modal periods is observed, a fact that validates the adequacy of the structural model at least for static and small intensity dynamic loads.

Mode	Period (sec)	Ux	Uy	Uz	Rx	Ry	Rz
1st	0,290(0.357)	0,73	1,845E-05	0,00012	0,0001	0,32	0,357
2nd	0,263(0.329)	8,18E-08	0,78	0,00071	0,26612	3,9E-04	0,182
3rd	0,196	0,00861	0,00024	7,16E-06	3,82E-06	2,66E-03	0,200

Table 3. Modal periods and participating mass ratios for displacement (U) and rotation (R). In parentheses the corresponding measured values

The representative Figure 9 shows the stress distribution for a seismic combination. Deep blue (darkest color) indicates the areas where the developed stresses are greater than the tensile strength of masonry. A detailed presentation of the results and the corresponding figures are provided in [7]. It is worth noting that the analysis identified with good accuracy the areas where critical damages were identified from the visual inspection.
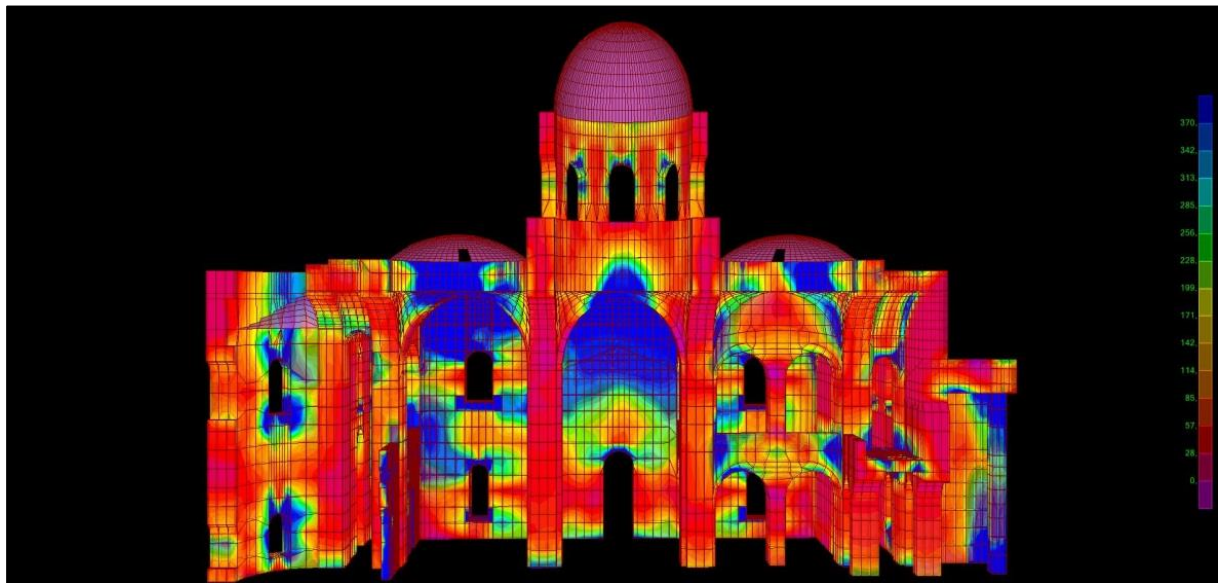
Figure 9. Stress distribution S22 for the $E_x+0.3E_y+0.3E_z$ combination

3.2 Local Analysis

The observation of the damages on churches struck by major earthquakes has revealed that this type of structures can be analyzed as a set of architectural parts characterized by a structural response basically independent from the church as a whole. These parts, referred to as macroelements, can be identified depending on the architectural and structural features of a church, such as the façade, the apse, the bell tower, the dome, the triumphal arch, etc. [8].

For each macroelement, a kinematic limit analysis is performed. Dealing with damaged churches, the uncertainties in choosing, a priori, the collapse mechanism are usually very small, since an accurate survey of the damages can lead to an "understanding" of their structural behavior. Moreover, a systematic analysis of the construction details, such as the masonry typology or the presence of earthquake-resistant elements, can help to identify the macroelements and to forsee which collapse mechanism is more likely to develop.

In addition to the kinematic approach, another feasible way to evaluate the seismic resistance of a macroelement, without choosing a priori the collapse mechanism, is to perform a non-linear static analysis by means of a finite element model.

A realistic approach to analyze these systems is to model the arches as a set of blocks and joints. The approach is known as the "blocks and joints" method [9]. As shown in Figure 10, both blocks and joints are frame elements: the blocks have the mechanical properties of the stone and their cross section is the effective cross section of the arch, the joints represent the mortar between the blocks. Four joints for each block are used; therefore, the joint cross section is ¼ of the arch cross section. The joints have a pin-end and a fixed-end, the fixed-end provides continuity with the previous block, the pin-end transfers shear and axial force to the next block, while the joints are connected to the block ends through rigid links; in this manner the system transfers moment, shear and axial force from one block to another.
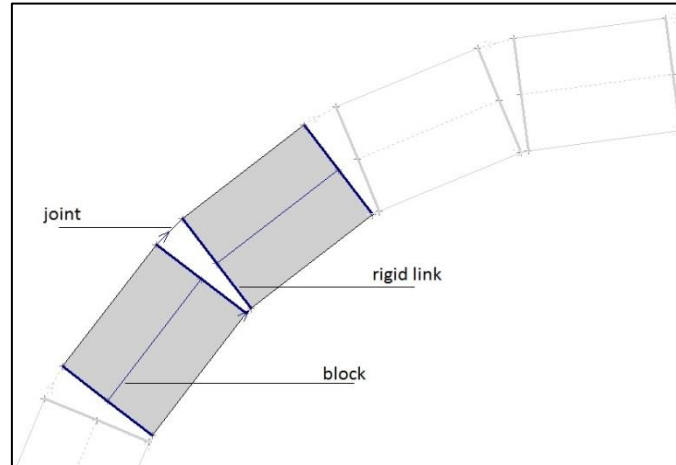
Figure 10. Structural model of an arch

When performing a pushover analysis, an axial force verification is applied to the joints, that is: if the tensile stresses exceed resistance, the fixed-end is turned to pin and the axial force is released so that the element loses any stiffness and the internal actions remain constant at the value reached so far. As the analysis continues, the progressive deterioration of the joints lead to an unstable configuration that define the end of the pushover curve.

The pillars are also divided into blocks and modeled with frame elements. At each step of the pushover analysis, the blocks are subjected to verification in terms of compression, that is examination of the thrust line position. If the thrust line comes out of the section of the block, a plastic hinge develops at the relevant node. The incremental analysis continues until the structure becomes unstable determining the maximum lateral force that the system can sustain.

The aim of non-linear static analysis applied to a *"blocks and joints"* system and to the masonry pillars is to determine the collapse multiplier α_0, that is given by

$$\alpha_0 = \frac{F_{max}}{W} \tag{9}$$

where F_{max} is the maximum lateral force that the structure can sustain and W is the total weight of the structure.

It should be pointed out that the "blocks and joints" analysis resembles to a kinematic analysis; however, the collapse multiplier is pursued as the maximum static multiplier instead of the minimum kinematic multiplier.

The spectral acceleration that activates the mechanism can be calculated as follows:

$$\alpha_0^* = \frac{\alpha_0 \cdot g}{e^* \cdot CF} \tag{10}$$

where g is the gravity acceleration, e^* is the participating mass ratio, CF is the confidence factor related to a limit knowledge level (KL1): thus equal to 1.35 [10, 11].
The participating mass and the participating mass ratios can be obtained from the following formulas considering the virtual displacement of the nodes where the weight is applied

$$M^* = \frac{(\sum P_i \delta_{x,i})^2}{g \cdot \sum P_i \delta_{x,i}^2} \tag{11}$$

$$e^* = \frac{g \cdot M^*}{\sum P_i} \tag{12}$$

where P_i is the weight applied to node i of the structure, $\delta_{x,I}$ is the virtual horizontal displacement of node i at the ultimate limit state.

The analyzed macroelement consists of three arches and four piers arranged along an alignment in the transverse direction of the church. The model and the analysis were performed with the aid of the software Aedes PC.E [9]. The model shown in Figure 11 consists of 604 frame elements and 488 nodes. For each node the rotation around the vertical Z axis is restrained, while the nodes at the base of the piers are fully fixed.
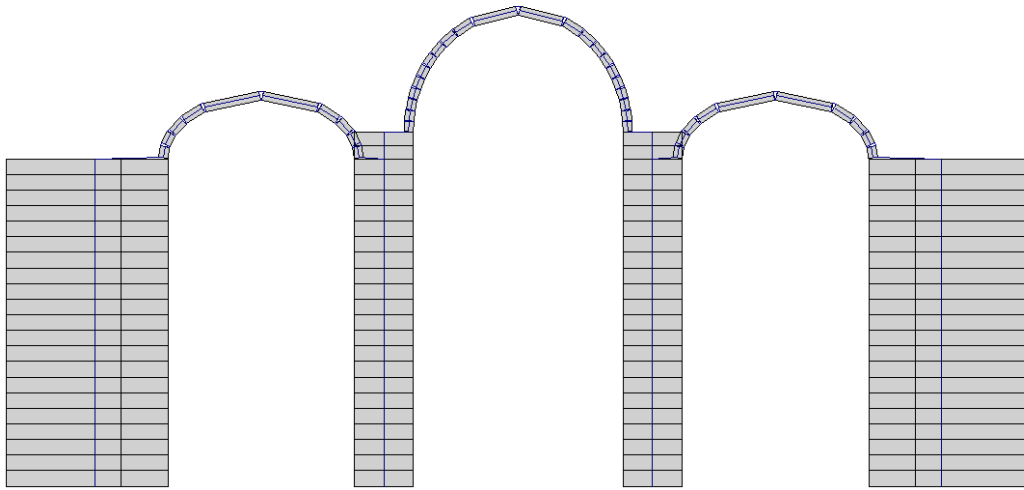

Figure 11. Structural model of the analyzed macroelement

To account for the weight of the structure that was not included in the model, vertical point loads have been applied at the top nodes of the piers. Their values were calculated in order to cause a vertical reaction at the base of the pier equal to the one found with the global model of the church; thus, vertical loads of *1890 kN* and *1570 kN* were applied on a lateral pier and a central one, respectively. The total weight of the structure is *W = 11105 kN*.

Figure 12 shows the deformed shape of the first mode of vibration, with the red spheres representing the mass associated to each node. The fundamental period of the structure is *0.544s* and the associated participating mass is *58%* as obtained from modal analysis.
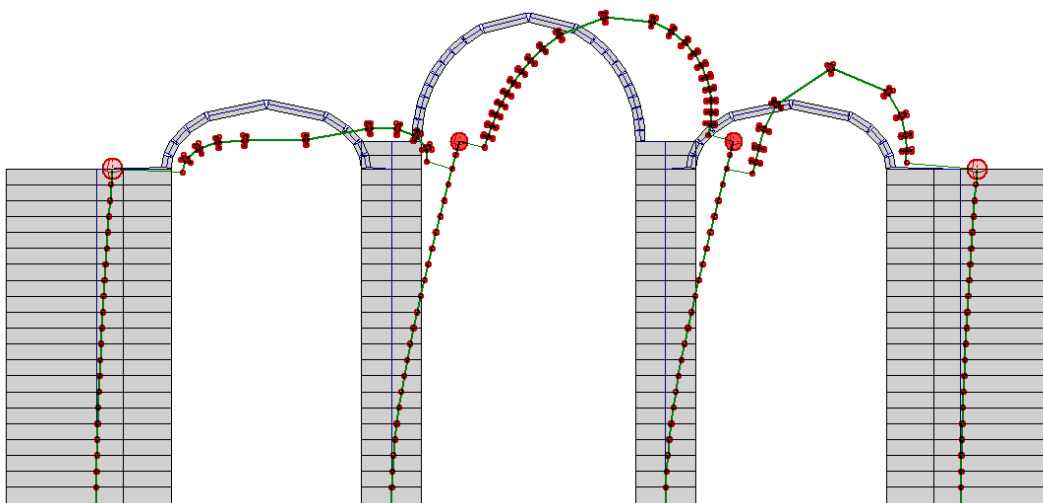

Figure 12. Deformed shape of the fundamental mode of vibration

The pushover analyses were performed using two lateral load distributions: (i) a "triangular" distribution (A) with lateral forces proportional to mass and elevation; and (ii) a "uniform" distribution (B) with lateral forces proportional to mass regardless of elevation.

Figure 13 shows the capacity curves of the structure at the initial state, obtained for the load distributions A and B. In the first case the structure reaches an unstable configuration for a lateral force equal to 600 kN, while with the load distribution B the maximum lateral force the structure can sustain is 750 kN.
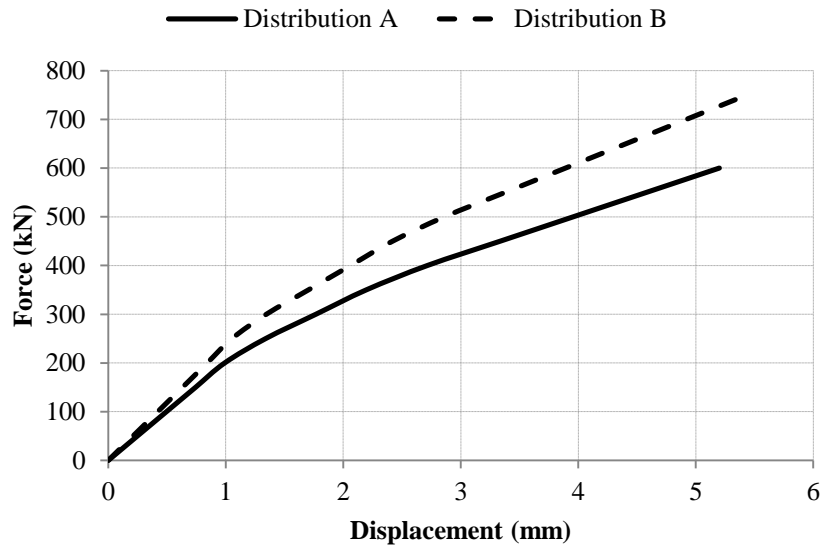

Figure 13. Capacity curves of the structure at initial state

The results from the "triangular" distribution of the lateral forces, being more severe, will be used for safety evaluation of the structure. Figure 14 shows the deformed shape and the position of the pressure curve at the last step of the pushover analysis for the distribution A.
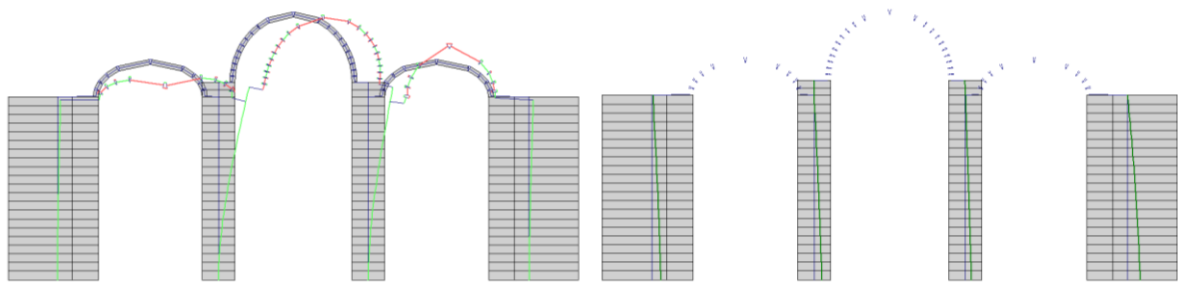

Figure 14. a) Deformed shape and b) pressure curve at last step of curve A

The deformed shape reveals the position of the plastic hinges that developed in the arches for joint degradation between the blocks. The pressure curve remains internal to the cross section of the piers; therefore, no plastic hinges develop in that area.

The collapse multiplier obtained from the analysis is

$$\alpha_0 = \frac{F_{max}}{W} = \frac{600}{11105} = 0.054 \qquad (13)$$

The participating mass ratio was calculated from Equation (12) to be $e^*=0.487$. Therefore, use of Equation (10) led to the acceleration that activates the mechanism

$$\alpha_{0,1}^* = \frac{\alpha_0 \cdot g}{e^* \cdot CF} = \frac{0.054}{0.487 \cdot 1.35} \cdot g = 0.082 \ g \tag{14}$$

The ultimate limit state is reached if the spectral acceleration

$$\alpha_0^* \geq \frac{\alpha_g \cdot S}{q} = \frac{0.16g \cdot 1.2}{1.5} = 0.128 \ g \tag{15}$$

where $a_g = 0.16g$ is the design ground acceleration for ground type A, $S = 1.2$ is the soil factor and $q = 1.5$ is the behavior factor.

For the structure at the initial state, $\alpha_{0,1}^*$ calculated from Equation (14) does not satisfy Equation (15); therefore, the structure does not reach the ultimate limit state. The maximum ground acceleration that it can sustain is

$$\alpha_{g,max,1} = \alpha_{0,1}^* \cdot q/S = 0.103g \tag{16}$$

4 RETROFIT AND STRENGTHENING MEASURES

According to the results of the analysis and the architectural restrictions imposed by the authorities that require minimum intervention to the structural configuration of the historic building and its decorated walls, the rehabilitation and strengthening of the church was based on a combined scheme using (a) grout injections, (b) CFRP and (c) steel tie-rods that complied with all limitations [12, 13]. The scheme is briefly described in the following.

According to international practice for seismic strengthening of three-leaf masonry walls, consolidation of masonry walls can be accomplished with grout injection characterized by grouts with a compressive strength in the range of 10 MPa. A compressive strength of 10 MPa was used in the analysis for the injected material which, combined with strength of the stones, determined the strength of the wall according to [14]

$$f_{wc,s} = f_{wc,0} + 0.31(V_{inf}/V)f_{gr}^{1,18} \tag{17}$$

where $f_{wc,S}$ is the compressive strength before grout injection, $f_{wc,0}$ is the compressive strength before grout injection, V_{inf}/V is ratio of grout volume to masonry volume, f_{gr} is the compressive strength of the grout. Application of Equation (17) led to Table 4.

		At initial state	After interventions	
Modulus of Elasticity	E	3710	5600	N/mm^2
Compressive strength	f$_c$	3.71	5.60	N/mm^2
Tensile strength	f$_t$	0.37	0.56	N/mm^2

Table 4. Mechanical characteristics of masonry

The tensile strength and stiffness of the exterior surface of the roof, as well as parts of the interior surfaces of certain vaults that are not decorated with historic paintings, was increased by applying sheets of carbon fiber impregnated with inorganic resins [15]. Specifically either three or two-plies of carbon fiber sheets (CFRP), with carbon sheet thickness of 0.17 mm per ply, were selected. The mechanical properties of the carbon fiber are: modulus of elasticity $E_c = 240 \ GPa$ and ultimate strength $f_j = 3500 \ MPa$.

Also stainless steel tie-rods F430 with a diameter of 40mm were placed at the upper part of the arches in the interior of the church. The mechanical properties of the tie-rods are: modulus of elasticity $E_c = 200 \ GPa$, yield strength $f_y = 379 \ MPa$ and ultimate strength $f_u = 552 \ MPa$.

Figure 15. Position of the steel tie-rods

The results of modal analysis for the first three modes of the strengthened structure and the modal participating mass ratios are listed in Table 5.

Mode	Period (sec)	Ux	Uy	Uz	Rx	Ry	Rz
1st	0,186	7,508E-07	0,594	0	0,875	1,102E-6	0,206
2nd	0,186	0,594	7,508E-07	0	1,102E-6	0,875	0,205
3rd	0,124	2,561E-09	2,554E-09	0	3,736E-09	3,745E-09	0,189

Table 5. Modal periods and participating mass ratios from global modal analysis

Comparison between Table 3 and Table 5 clearly indicates the decrease of the modal periods after the interventions. According to the results of response spectrum analysis applied to the strengthened structure, it was observed that excess of the tensile strength (10% of the compressive strength of masonry) is limited at "secondary" places of the masonry walls for the seismic load combinations. Figure 16 showing the stresses after interventions corresponds to Figure 9.
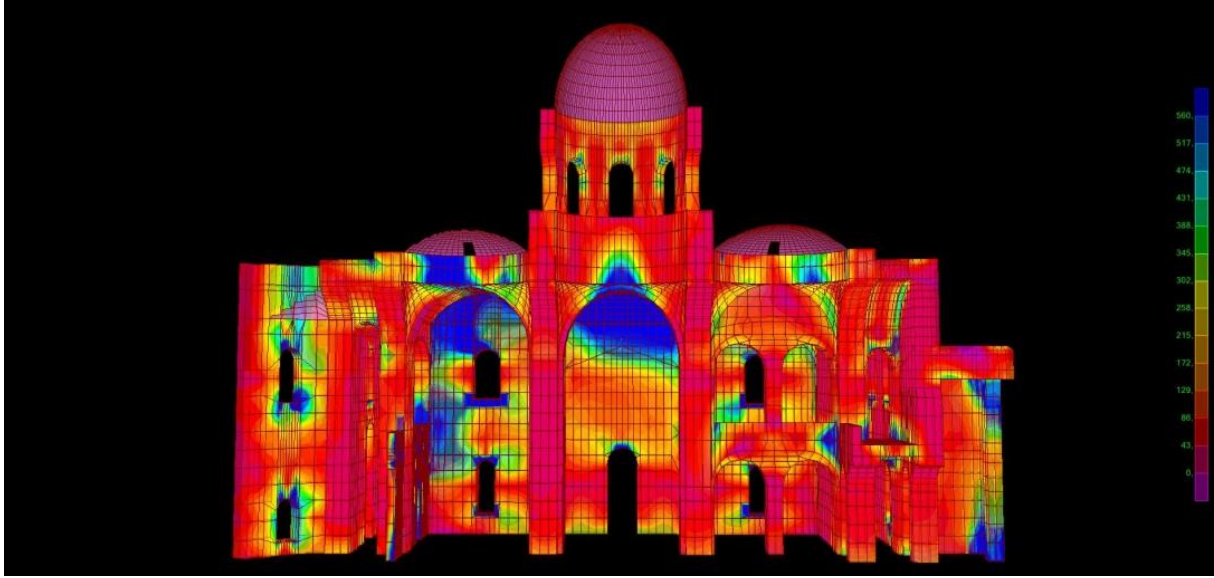
Figure 16. Stress distribution S22 for the $E_x+0.3E_y+0.3E_z$ combination

Local analysis provided that after the interventions the collapse multiplier is

$$\alpha_0 = \frac{F_{max}}{W} = \frac{1200}{11105} = 0.108 \tag{18}$$

The participating mass ratio calculated according to Equation (12) is $e^* = 0.657$. Therefore, the acceleration that activates the mechanism, calculated from Equation (10) is

$$\alpha_{0,2}^* = \frac{\alpha_0 \cdot g}{e^* \cdot CF} = \frac{0.108}{0.465 \cdot 1.35} \cdot g = 0.172 \; g \tag{19}$$

Since $\alpha_{0,2}^*$ satisfy Equation (15), the structure reaches the ultimate limit state and the maximum ground acceleration that it can sustain is:

$$\alpha_{g,max,1} = \alpha_{0,2}^* \cdot q/S = 0.175g \tag{20}$$

5 CONCLUSIONS

A series of tests were performed to the historic church of St. Nicholas in Piraeus. Besides the visual inspections, in-situ and laboratory testing as well as ambient vibration testing provided the mechanical characteristics of the materials and the dynamic characteristics of the church as a whole.

Three types of analysis were conducted: (i) modal analysis that was validated through ambient vibration measurements; (ii) response spectrum analysis based on the current Eurocode provisions; (iii) local analysis using a "block and joints" model. All analyses were performed in order to evaluate the response of the structure prior and after interventions.

It was ascertained: (i) the seismic risk of the church prior to interventions, and (ii) the effectiveness of the proposed strengthening measures, that is, consolidation of the walls through grouting, use of CFRP with inorganic resins and steel tie-rods.

Combination of the intervention technics dramatically enhanced the seismic safety of the structure and fulfilled the historic preservation mandates.

REFERENCES

[1] Σ.Γ. Μαλικούτη, *Πειραιάς 1834-1912. Λειτουργική συγκρότηση και πολεοδομική εξέλιξη*. Πολιτιστικό Ίδρυμα Ομίλου Πειραιώς, Αθήνα, 2004. (in Greek)

[2] Θ.Π. Τάσιος, Μ.Π. Χρονόπουλος, *Παθολογικά Αίτια και Μηχανική των Βλαβών της Τοιχοποιίας*. Υ.ΠΕ.ΧΩ.ΔΕ. Εργ. Ωπλ. Σκυροδέματος Ε.Μ.Π., Αθήνα, 1986. (in Greek)

[3] SAP2000, 14.0.0, Computers and Structures Inc, Berkeley, California, 2009.

[4] C.C. Spyrakos, *Finite Element Modeling in Engineering Practice*. Algor Publishing Division, Pittsburg, PA, USA, 1995.

[5] EN 1998-1:2005. Eurocode 8: Design of structures for earthquake resistance - Part 1: General rules, seismic action and rules for buildings, CEN, 2005.

[6] EN 1998-3:2005. Eurocode 8: Design of structures for earthquake resistance - Part 3: Assessment and retrofitting of buildings, CEN, 2005.

[7] Σ. Παπουτσέλης, *Δομική Αποκατάσταση και Στατική Στερέωση του Ιερού Ναού Αγίου Νικολάου Πειραιώς*, Σχολή Πολιτικών Μηχαωικών, Εθνικό Μετσόβιο Πολυτεχνείο, 2012. (in Greek)

[8] D.P.C.M 9 febbraio 2011. Linee guida per la valutazione e la riduzione del rischio sismico del patrimonio culturale con riferimento alle Norme tecniche per le costruzioni di cui al D.M. 14/01/2008, 2011. (in Italian)

[9] PC.E, 2012.04.1, Aedes Software snc, Pisa, 2012.

[10] Circolare 2 febbraio 2009, n. 617. Istruzioni per l'applicazione delle "Nuove norme tecniche per le costruzioni" di cui al D.M. 14 gennaio 2008, 2009. (in Italian)

[11] D.M. 14 gennaio 2008. Nuove norme tecniche per le costruzioni, 2008. (in Italian)

[12] Κ. Σπυράκος, *Ενίσχυση Κατασκευών για Σεισμικά Φορτία*. Τεχνικό Επιμελητήριο Ελλάδας, Αθήνα, 2004. (in Greek)

[13] P. Foraboschi, Strengthening of masonry arches with fiber-reinforced polymer strips. *Journal of Composites for Construction*, **8**, 191-202, 2004.

[14] M.R. Valluzzi, F. Da Porto, C. Modena, Behavior and modeling of strengthened three-leaf stone masonry walls. *Materials and Structures/Materiaux et Constructions*, **37**, 184-192, 2004.

[15] L. Credali, G. Ussia, Composite Materials Technologies in Constructions Structural Retrofitting: New Developments and Applications in Historical Buildings and Applications in Seismic Zone. *COMPDYN 2011 3rd International Conference on Computational Methods in Structural Dynamics and Earthquake Engineering*, Corfu, Greece, May 25-28, 2011.

[16] C.C. Spyrakos, P.D. Kiriakopoulos, E. Smyrou, Seismic Strengthening of the Historic Church of Sts Helen and Constantine in Piraeus. *COMPDYN 2011 3rd International Conference on Computational Methods in Structural Dynamics and Earthquake Engineering*, Corfu, Greece, May 25-28, 2011.

[17] F. Pugi, *Edifici in Muratura e nuova Normativa Sismica: l'Analisi Pushover come evoluzione del Metodo Por*. Alinea, Firenze, 2006. (in Italian)

[18] P. Lenza, A. Ghersi, B. Calderoni, *Edifici in muratura alla luce della nuova normativa sismica*. D. Flaccovio, Palermo, 2011. (in Italian)

[19] M. Corradi, A. Borri, A. Vignoli, Strengthening techniques tested on masonry structures struck by the Umbria–Marche earthquake of 1997–1998. *Construction and Building Materials*, **16**, 229-239, 2002.

[20] P.B. Lourenço, Assessment, diagnosis and strengthening of Outeiro Church, Portugal. *Construction and Building Materials*, **19**, 634-645, 2005.